9554 *Inorg. Chem.* **2010**, *49*, 9554–9562
DOI: 10.1021/ic101251a

Inorganic Chemistry
Article

The Reaction Chemistry of Plutonyl(VI) Chloride Complexes with Triphenyl Phosphineoxide and Triphenyl Phosphinimine†

Claude Berthon,[#] Nathalie Boubals,[#] Iraida A. Charushnikova,[#] David Collison,[‡] Stéphanie M. Cornet,[*,§] Christophe Den Auwer,[#] Andrew J. Gaunt,[∥] Nikolas Kaltsoyannis,[*,⊥] Iain May,[*,∥] Sebastien Petit,[§] Michael P. Redmond,[§] Sean D. Reilly,[∥] and Brian L. Scott[▽]

[#]*CEA, Nuclear Energy Division, RadioChemistry and Process Department, F-30207 Bagnols sur Cèze, France,* [‡]*School of Chemistry, The University of Manchester, Manchester M13 9PL, U.K.,* [§]*Centre for Radiochemistry Research, School of Chemistry, The University of Manchester, Manchester M13 9PL, U.K.,* [∥]*Chemistry Division, Inorganic, Isotope and Actinide Chemistry (C-IIAC), Los Alamos National Laboratory, Mail Stop J-514, Los Alamos, New Mexico 87545,* [⊥]*Department of Chemistry, University College London, 20 Gordon Street, London WC1H 0AJ, U.K., and* [▽]*Materials and Physics Applications − Materials Chemistry (MPA-MC), Los Alamos National Laboratory, Mail Stop J-514, Los Alamos, New Mexico 87545*

Received June 23, 2010

The reaction between Ph_3PO dissolved in acetone and "PuO_2Cl_2" in dilute HCl resulted in the formation of $[PuO_2Cl_2(Ph_3PO)_2]$. Crystallographic characterization of the acetone solvate revealed the expected axial *trans* plutonyl dioxo, with *trans* Cl and Ph_3PO in the equatorial plane. Spectroscopic analyses (^{31}P NMR, ^{1}H NMR, and vis/nIR) indicate the presence of both *cis* and *trans* isomers in solution, with the trans isomer being more stable. Confirmation of the higher stability of the *trans* versus *cis* isomers for $[AnO_2Cl_2(Ph_3PO)_2]$ (An = U and Pu) was obtained through quantum chemical computational analysis, which also reveals the $Pu-O_{TPPO}$ bond to be more ionic than the $U-O_{TPPO}$ bond. Slight variation in reaction conditions led to the crystallization of two further minor products, $[PuO_2(Ph_3PO)_4][ClO_4]_2$ and *cis*-$[PuCl_2(Ph_3PO)_4]$, the latter complex revealing the potential for reduction to Pu^{IV}. In addition, the reaction of Ph_3PNH with $[PuO_2Cl_2(thf)_2]_2$ in anhydrous conditions gave evidence for the formation of both *cis*- and *trans*-$[PuO_2Cl_2(Ph_3PNH)_2]$ in solution (by ^{31}P NMR). However, the major reaction pathway involved protonation of the ligand with the crystallographic characterization of $[Ph_3PNH_2]_2[PuO_2Cl_4]$. We believe that $HCl/SiMe_3Cl$ carried through from the small scale preparation of $[PuO_2Cl_2(thf)_2]_2$ was the source of both protons and chlorides. The fact that this chemistry was significantly different from previous uranium studies, where *cis*-/*trans*-$[UO_2Cl_2L_2]$ (L = Ph_3PO or Ph_3PNH) were the only products observed, provides further evidence of the unique challenges and opportunities associated with the chemistry of plutonium.

Introduction

An increased understanding of the fundamental coordination chemistry of plutonium will yield essential underpinning knowledge for a range of applied nuclear processes including decommissioning, stockpile stewardship, safe long-term nuclear waste storage and environmental management. In addition, the increased interest in nuclear power as a non-carbon-based source of energy will only enhance our need to develop novel chemical/material processes for actinide (including plutonium) separations and the development of advanced fuel types. However, the radiological toxicity of plutonium greatly restricts the number of laboratories that are able to undertake this type of research, limiting progress. In addition, the chemistry of plutonium is uniquely complex with six accessible oxidation states (0, III, IV, V, VI, and VII), four of which can coexist in aqueous solution.[1]

The linear dioxo actinyl moieties, $\{AnO_2\}^+$ and $\{AnO_2\}^{2+}$, dominate the coordination chemistry of the +V and +VI oxidation state mid-actinide elements (U, Np, Pu, and Am).[1,2]

† Dedicated to the memory of J. P. Day (School of Chemistry, The University of Manchester).

*To whom correspondence should be addressed. E-mail: stephanie.cornet@manchester.ac.uk, n.kaltsoyannis@ucl.ac.uk, iainmay@lanl.gov.

(1) Clark, D. L.; Hecker, S.; Jarvinen, G. D.; Neu, M. P. In *The Chemistry of the Actinide and Transactinide Elements*; Morss, L. R., Edelstein, N. M., Fuger, J., Eds.; Springer: Dordrecht, The Netherlands, 2006; Vol. 2, Chapter 7, pp 813−1264.

(2) (a) Grenthe, I.; Drożdżyński, J.; Fujino, T.; Buck, E. C.; Albrecht-Schmitt, T. E.; Wolf, S. F. In *The Chemistry of the Actinide and Transactinide Elements* Morss, L. R., Edelstein, N. M., Fuger, J., Eds.; Springer: Dordrecht, The Netherlands, 2006; Vol. 1, Chapter 5, pp 253−698. (b) Yoshida, Z.; Johnson, S. G.; Kimura, T.; Krsul, J. R. In *The Chemistry of the Actinide and Transactinide Elements*; Morss, L. R., Edelstein, N. M., Fuger, J., Eds.; Springer: Dordrecht, The Netherlands, 2006; Vol. 2, Chapter 6, pp 699−812. (c) Runde, W. H.; Wallace, W. S. In *The Chemistry of the Actinide and Transactinide Elements* Morss, L. R., Edelstein, N. M., Fuger, J., Eds.; Springer: Dordrecht, The Netherlands, 2006; Vol. 2, Chapter 8, pp 1265−1396. (d) Denning, R. G. *J. Phys. Chem. A* **2007**, *111*, 4125.

 Published on Web 09/14/2010

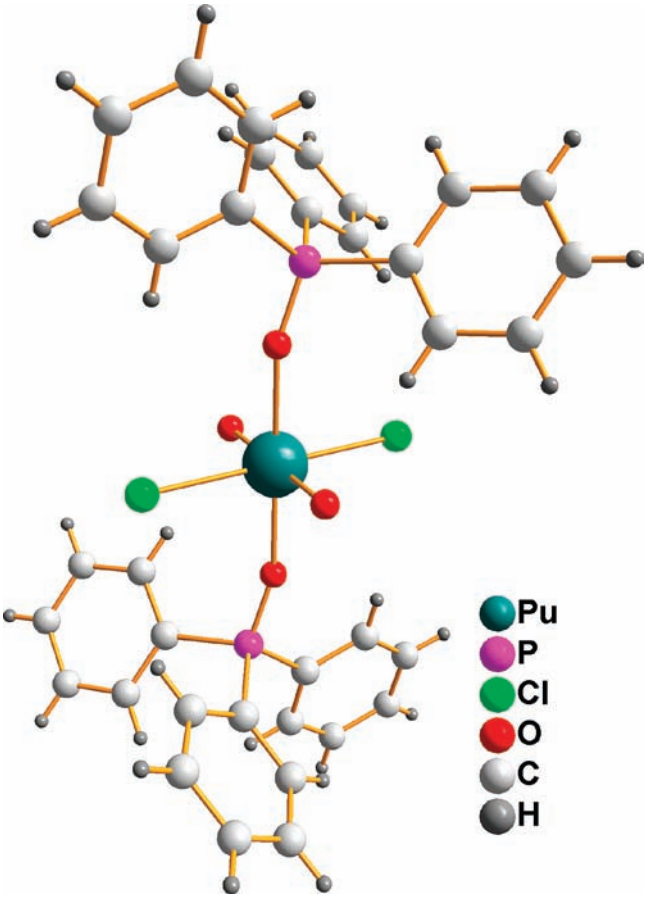

Figure 1. Ball and stick representation of *trans*-$[PuO_2Cl_2(Ph_3PO)_2]$.

Typically between four and six additional ligands occupy the equatorial plane. In the case of uranium, the comparative ease of access, lower radioactive hazards, and high stability of the +VI oxidation state has allowed the uranyl moiety to be studied in great detail.[3] Reports on the chemistry of the transuranic actinyls tend to drop off with decreasing chemical stability and/or decreasing radioactive half-lives of the major isotopes. A similar story emerges from computational studies where the closed-shell $5f^0$ uranyl(VI) moiety is far easier to study than the remaining open-shell actinyl moieties, all of which possess 5f valence electrons.[4]

Previously we have probed bonding in the uranyl(VI) and neptunyl(VI) equatorial plane through the tetragonal bipyramidal complexes of general formula $[AnO_2Cl_2L_2]$, where An = U or Np and L = phosphineoxide (R_3PO) or phosphinimine (R_3PNH).[5,6] During the course of these experimental investigations, we observed that *trans* coordination in the equatorial plane was more stable than *cis* coordination and that the more basic phosphinimine ligands would more strongly coordinate to the actinyl center than the corresponding phosphineoxide ligands. In the case of uranyl, we determined, through computational techniques, that stronger phosphinimine coordination was due to a significant covalent bonding interaction.[6] This was a rather unusual observation because covalency in the bonding of actinyl complexes is usually focused within the linear O=An=O bonds.[2] We now report our attempts to extend this study to plutonyl(VI) through the reaction of aqueous plutonyl(VI) chloride with Ph_3PO (TPPO) and the anhydrous plutonyl complex $[PuO_2Cl_2(thf)_2]_2$ with moisture-sensitive Ph_3PNH.

Results and Discussion

$[PuO_2Cl_2(Ph_3PO)_2]$ could readily be prepared from the reaction of an acidic aqueous "PuO_2Cl_2" solution, and Ph_3PO dissolved in acetone. *trans*-$[PuO_2Cl_2(Ph_3PO)_2]\cdot 2(CH_3)_2CO$ could be crystallized from an aqueous acetone solution, revealing a six-coordinate Pu^{VI} complex with the expected *trans* configuration of the dioxo 'yl' ligands and the two chloride and two P=O (Ph_3PO) donor ligands occupying *trans* positions around the plutonyl equatorial plane (see Figure 1). The Pu atom sits at an inversion center, with the ligand−Pu−ligand bond angles indicative of almost perfect tetragonal bipyramidal symmetry.

Previously α-*trans*-$[UO_2Cl_2(Ph_3PO)_2]$, *β*-*trans*-$[UO_2Cl_2(Ph_3PO)_2]$, *trans*-$[NpO_2Cl_2(Ph_3PO)_2]$, and *cis*-$[UO_2Cl_2(Ph_3PO)_2]$ have all been structurally characterized, and the bond lengths are comparable for all five $[AnO_2Cl_2(Ph_3PO)_2]$ complexes (see Table 1).[7−9] In addition, the plutonyl bond length (1.747(4) Å) comes within the range previously observed for plutonyl(VI) complexes (1.69−1.77 Å),[10−14] and the Pu−Cl bond length (2.630(2) Å) is only slightly shorter than the value observed for $Cs_2[PuO_2Cl_4]$ (2.6648(8) Å).[12] The $Pu-O_{TPPO}$ bond length in *trans*-$[PuO_2Cl_2(Ph_3PO)_2]$ (2.302(4) Å) is comparable to the $Pu-O_{TPPO}$ bond lengths in $[PuO_2(Ph_3PO)_4](ClO_4)_2$ (2.299(4) and 2.276(3) Å).[13] The longer $Pu-O_{TPPO}$ bond length in $[PuO_2(NO_3)_2(Ph_3PO)_2]$ (2.353(2) Å) is almost certainly due to the greater steric constraints in this eight-coordinate complex (versus a coordination number of 6 for the other Pu^{VI} complexes).[14]

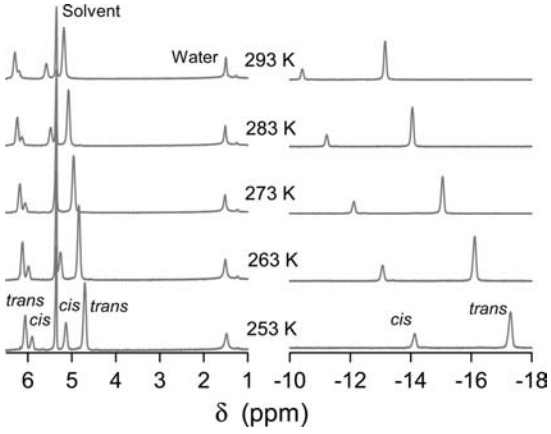

Figure 2. Variable-temperature ^1H NMR spectrum of crystalline $[PuO_2Cl_2(Ph_3PO)_2]$ (recrystallized from CH_2Cl_2) dissolved in CD_2Cl_2 with probable *cis*/*trans* assignments.

(3) (a) Ephritikhine, M. *Dalton Trans* **2006**, 2501. (b) Burns, C. J.; Neu, M. P.; Boukhalfa, H.; Gutowski, K. E.; Bridges, N. J.; Rogers, R. D. In *Comprehensive Coordination Chemistry II*; McCleverty, J. A., Meyer, T. J., Eds.; Elsevier Ltd.: Amsterdam, 2004; Vol. 3.3, p 189.

(4) Kaltsoyannis, N.; Hay, P. J.; Li, J.; Baludeau, J.-P.; Bursten, B. E. In *The Chemistry of the Actinide and Transactinide Elements* Morss, L. R., Edelstein, N. M., Fuger, J., Eds.; Springer: Dordrecht, The Netherlands, 2006; Vol. 3, Chapter 17, pp 1893−2012.

(5) Sarsfield, M. J.; May, I.; Cornet, S. M.; Helliwell, M. *Inorg. Chem.* **2005**, *44*, 7310.

(6) Häller, L. J. L.; Kaltsoyannis, N.; Sarsfield, M. J.; May, I.; Cornet, S. M.; Redmond, M. P.; Helliwell, M. *Inorg. Chem.* **2007**, *46*, 4868.

(7) Alcock, N. W.; Roberts, M. M.; Brown, D. *J. Chem. Soc., Dalton Trans.* **1982**, 25.

Table 1. Selected Bond Lengths (Å) for $[AnO_2Cl_2(Ph_3PO)_2]$ Complexes

complex	ref	bond			
		An−O_{yl}	An−O_{TPPO}	An−Cl	P−O
trans-$[PuO_2Cl_2(Ph_3PO)_2]$	this work	1.747(4)	2.302(4)	2.630(2)	1.505(4)
trans-$[NpO_2Cl_2(Ph_3PO)_2]$	7	1.751(18)	2.288(15)	2.622(14)	1.50(1)
		1.721(16)	2.261(16)	2.645(13)	1.55(2)
α-*trans*-$[UO_2Cl_2(Ph_3PO)_2]$	8	1.764(9)	2.300(8)	2.645(5)	1.518(8)
β-*trans*-$[UO_2Cl_2(Ph_3PO)_2]$	9	1.753(12)	2.306(12)	2.673(4)	1.535(3)
		1.767(12)	2.339(12)	2.657(4)	1.4677(12)
cis-$[UO_2Cl_2(Ph_3PO)_2]$	9	1.771(4)	2.340(4)	2.641(2)	1.524(4)

The ^1H and ^{31}P NMR spectra of $[PuO_2Cl_2(Ph_3PO)_2]$ recrystallized from CH_2Cl_2 and then dissolved in CD_2Cl_2 reveal features that are characteristic of two complexes in which Ph_3PO ligands are coordinated to a paramagnetic metal center (i.e., $5f^2$ Pu^{VI}). In the case of the ^1H NMR spectra, two sets of three resonances would appear to relate to the ortho, meta, and para protons on Ph_3PO, with increasing shift upfield with proximity to the paramagnetic plutonium center (see Figure 2). A similar splitting pattern was observed for $[NpO_2Cl_2(Ph_3PO)_2]$, although the extent of paramagnetic upfield shifting of the resonances was less pronounced for this $5f^1$ Np^{VI} complex.[5] Variable-temperature measurements reveal upfield shifts for all six resonances as the temperature is lowered; the effect of temperature is more pronounced with increased proximity to the paramagnetic plutonium center. The peak at ca. 1.5 ppm is consistent with uncoordinated water, despite attempts to exclude moisture from the system, and does not vary with temperature. This indicates that water does not displace either TPPO or chloride ligands from coordination to the plutonyl(VI) dication.

The ^{31}P NMR spectra reveal two resonances far upfield from uncomplexed Ph_3PO (28 ppm),[15] and we assign the two resonances to *cis*- and *trans*-$[PuO_2Cl_2(Ph_3PO)_2]$ (Figure 3). Interestingly, only one resonance, was observed in the RT ^{31}P NMR of $[NpO_2Cl_2(Ph_3PO)_2]$ at 15 ppm, suggesting that in that particular case the chemical shifts of the two isomers are very similar.[5] Variable-temperature measurements are consistent with the ^1H NMR data, the peak positions shifting upfield with decrease in temperature. Peak broadening as the temperature is lowered gives evidence for isomer exchange on the NMR time scale, while the relative intensity of the peak we assign to the *trans* isomer appears to decrease with temperature. It should also be noted that two resonances in the same spectral region could also be observed if there was no attempt to exclude moisture from the solvent, again suggesting that H_2O does not effectively compete with Ph_3PO or Cl^- for coordination to $\{PuO_2\}^{2+}$.

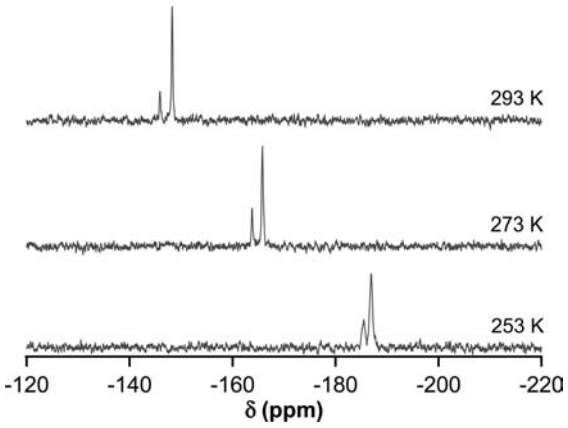

Figure 3. Variable-temperature ^{31}P NMR spectrum of $[PuO_2Cl_2(Ph_3PO)_2]$, recrystallized from CH_2Cl_2, dissolved in CD_2Cl_2; the major peak is assigned to the *trans* species.

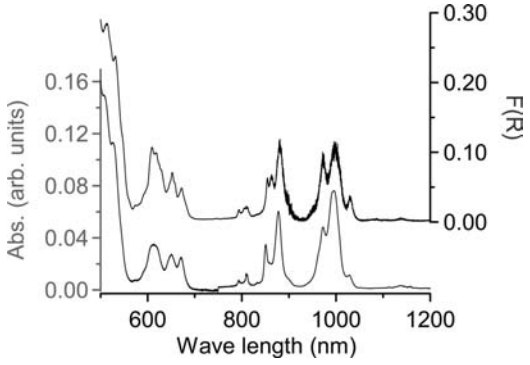

Figure 4. Vis/nIR spectrum of crystalline [*trans*-$PuO_2Cl_2(Ph_3PO)_2$] (diffuse reflectance, black spectrum and right axis) and a solution of $[PuO_2Cl_2(Ph_3PO)_2]$ in CH_2Cl_2 (gray spectrum, left axis).

Based on our results for the analogous uranyl(VI) complexes,[6] we would expect the major NMR resonances for $[PuO_2Cl_2(Ph_3PO)_2]$ to correspond to the *trans* isomer. Vis/nIR spectra were recorded for both $[PuO_2Cl_2(Ph_3PO)_2]$ in the solid state and a sample of the same material dissolved in dry CH_2Cl_2 (Figure 4). The spectra are very similar, indicative of a similar coordination environment around the Pu^{VI} center in both the solid state and solution. Minor differences can, in part, be attributed to the lower spectral peak to noise ratio at lower energy (solid state) and lower peak resolution (solution state). However, there are also some subtle changes in peak intensities/positions, particularly between 800 and 900 nm, indicating some differences in speciation between solid state and solution.

(8) Bombieri, G.; Forsellini, E.; Day, J. P.; Azeez, W. I. *J. Chem. Soc., Dalton Trans.* **1978**, 677.
(9) Akona, S. B.; Fawcett, J.; Holloway, J. H.; Russel, D. R. *Acta Crystallogr.* **1991**, *C47*, 45.
(10) (a) Charushnikova, I. A.; Krot, N. N.; Polyakova, I. N.; Starikova, Z. A. *Radiochemistry* **2007**, *49*, 117. (b) Charushnikova, I. A.; Krot, N. N.; Starikova, Z. A. *Radiochemistry* **2007**, *49*, 565. (c) Bean, A. C.; Abney, K.; Scott, B. L.; Runde, W. *Inorg. Chem.* **2005**, *44*, 5209. (d) Bean, A. C.; Scott, B. L.; Albrecht-Schmitt, T. E.; Runde, W. R. *J. Solid State Chem.* **2004**, *177*, 1346. (e) Grigoriev, M. S.; Antipin, M.Yu.; Krot, N. N.; Bessonov, A. A. *Radiochim. Acta* **2004**, *92*, 405. (f) Copping, R.; Talbot-Eeckelears, C.; Collison, D.; Helliwell, M.; Gaunt, A. J.; May, I.; Reilly, S. D.; Scott, B. L.; McDonald, R. D.; Valenzula, O. A.; Jones, C. J.; Sarsfield, M. J. *Dalton Trans.* **2009**, 5609–5611.
(11) Gaunt, A. J.; Reilly, S. D.; Hayton, T. W.; Scott, B. L.; Neu, M. P. *Chem. Commun.* **2007**, 1659.
(12) Wilkerson, M. P.; Scott, B. L. *Acta Crystallogr.* **2008**, *E64*, i5.
(13) Charushnikova, I. A.; Krot, N. N.; Starikova, Z. A.; Polyakova, I. N. *Radiochemistry* **2007**, *49*, 464.
(14) Charushnikova, I. A.; Krot, N. N.; Starikova, Z. A. *Radiochemistry* **2007**, *49*, 561.
(15) Albright, T. A.; Freeman, W. J.; Schweizer, E. E. *J. Org. Chem.* **1975**, *40*, 3437.

Table 2. Selected Calculated Bond Lengths (Å) and Angles (deg) for the *cis* and *trans* Forms of $[UO_2Cl_2(Ph_3PO)_2]$[a]

	trans, (g), scalar	*cis*, (g), scalar	*trans*, (g), SO	*cis*, (g), SO	*trans*, (s), scalar	*cis*, (s), scalar	*trans*, (s), SO
$r_{U-O_{yl}}$	1.805	1.805	1.806	1.807	1.810	1.807	1.812
r_{U-O}	2.405	2.456	2.391	2.441	2.359	2.375	2.345
r_{U-Cl}	2.644	2.616	2.635	2.606	2.661	2.650	2.652
r_{P-O}	1.525	1.529	1.526	1.528	1.537	1.537	1.538
$\alpha_{O_{yl}-U-O_{yl}}$	179.9	173.9	180.0	173.5	180.0	176.9	180.0
$\alpha_{Cl-U-Cl}$	180.0	96.3	179.9	96.4	179.8	90.2	179.9
α_{P-O-U}	147.5	138.0	147.4	139.3	155.4	146.5	154.4

[a] In each case, the bond length data are the average values of two bonds; (g) indicates isolated molecule, (s) indicates solvent-corrected molecule, SO indicates spin-orbit.

Focusing on the 800−900 nm region of the $[PuO_2Cl_2(Ph_3PO)_2]$ absorption spectra, we typically see a dominant very sharp and intense transition for $\{PuO_2\}^{2+}$, which is centered at 830 nm (ε 550) for $[PuO_2(H_2O)_5]^{2+}$.[16] The higher intensity of this formally Laporte forbidden transition ($^3H_{4g} \rightarrow {}^3\Pi_{2g}$) versus the other 5f−5f transitions has been attributed to the ligand field providing sufficient $5f^{\phi}$ and $6d^{\delta}$ mixing to relax the selection rule.[17] However, if the $5f^2$ Pu atom is at an inversion center then this transition should be completely forbidden. There is experimental evidence that this is the case with the solution spectrum for D_{3h} $[PuO_2(CO_3)_3]^{4-}$ (D_{6h} symmetry in the first coordination sphere) having no band between 800 and 900 nm with an intensity above ε 25.[18] More detailed studies have also been performed on neptunyl(V) $5f^2$ complexes, which show the disappearance or marked decrease in intensity of the $^3H_{4g} \rightarrow {}^3\Pi_{2g}$ transition (observed at 980 nm for $[NpO_2(H_2O)_5]^{+}$) for complexes with an inversion center.[19] For *cis*-/*trans*-$[PuO_2Cl_2(Ph_3PO)_2]$, only the *trans* isomer will have an inversion center at Pu, and if the *cis*-isomer dominated in solution or in the solid state, then an intense transition around 820−880 nm may be expected to dominate the spectra between 550 and 1200 nm, but this is not the case. Therefore, we believe that *trans*-$[PuO_2Cl_2(Ph_3PO)_2]$ is the major product in the solid state and that the *trans* isomer dominates in solution.

Gaunt et al. previously studied the reaction between $[PuO_2Cl_2(thf)_2]_2$ and various molar equivalents of Ph_3PO in thf by both ^{31}P NMR and UV/vis/nIR spectroscopy at room temperature.[11] They also observed resonance(s) between −140 and −150 ppm that can be attributed to *cis*- and *trans*-$[PuO_2Cl_2(TPPO)_2]$, with line broadening often obscuring the presence of more than one resonance. At lower $Ph_3PO/\{PuO_2\}^{2+}$ ratios another peak at −16 ppm was observed, which they assign to a $\{PuO_2\}^{2+}$ complex with one coordinated Ph_3PO. They also report a decrease in energy of the $^3H_{4g} \rightarrow {}^3\Pi_{2g}$ transition from 856 nm (for $[PuO_2Cl_2(thf)_2]_2$) to 879 nm on the addition of Ph_3PO, again assigned to a 1:1 $\{PuO_2\}^{2+}/Ph_3PO$ complex. Addition of more TPPO led to a dramatic decrease in intensity of this transition and an absorption spectra comparable to the one that we now report for $[PuO_2Cl_2(Ph_3PO)_2]$ in CH_2Cl_2. Higher ratios of TPPO were required to form this complex in thf than we observe in CH_2Cl_2, consistent with the ability of thf to compete with Ph_3PO for coordination to $\{PuO_2\}^{2+}$ (cf. noncoordinating CH_2Cl_2).

Table 3. Selected Calculated Bond Lengths (Å) and Angles (deg) for the cis and trans forms of $PuO_2Cl_2(Ph_3PO)_2$ [a]

	trans, (g)	cis, (g)	trans, (s)	cis, (s)
$r_{Pu-O_{yl}}$	1.773	1.769	1.775	1.773
r_{Pu-O}	2.393	2.415	2.347	2.366
r_{Pu-Cl}	2.619	2.613	2.637	2.634
r_{P-O}	1.525	1.528	1.534	1.537
$\alpha_{O_{yl}-Pu-O_{yl}}$	180.0	177.9	180.0	179.0
$\alpha_{Cl-Pu-Cl}$	179.8	93.9	180.0	88.9
α_{P-O-Pu}	145.6	136.9	154.3	140.0

[a] In each case, the bond length data are the average values of two bonds. All calculations are scalar; (g) indicates isolated molecule; (s) indicates solvent-corrected molecule.

The solid-state IR spectrum of $[PuO_2Cl_2(Ph_3PO)_2]$ was also recorded. Of most significance is the transition at 920 cm^{-1}, which we assign to the $O_{yl}{=}Pu{=}O_{yl}$ asymmetric stretch (υ_3). This value is comparable in energy to the equivalent vibrational transition in $(PuO_2)_2SiO_4 \cdot 2H_2O$ (916 cm^{-1}),[20] as well as in $[PuO_2Cl_2(dipy \cdot HCl)_2]$ (918 cm^{-1}), $[PuO_2Cl_2(phen \cdot HCl)_2]$ (912 cm^{-1}), and $[PuO_2Cl_2(dipy\text{-}O_2 \cdot HCl)_2]$ (908 cm^{-1}), where dipy = 2,2′-dipyridyl, phen = *o*-phenanthroline, and dipy-O_2 = 2,2′-dipyridyl-*N*,*N*′-dioxide.[21]

To support our experimental findings, we turned to computational methods that we have previously used to confirm the increased stability of *trans*-$[UO_2Cl_2(Cy_3PO)_2]$ versus *cis*-$[UO_2Cl_2(Cy_3PO)_2]$ in solution.[6] We have thus extended this study to Pu^{VI} and Ph_3PO (i.e., *cis*-/*trans*-$[AnO_2Cl_2(Ph_3PO)_2]$ where An = U/Pu), with selected calculated geometries presented in Tables 2 and 3. The structural calculations included a comparison of spin orbit versus scalar (U, isolated molecule, and also solvent corrected for the *trans* system only). No significant differences were observed, as might be expected for a closed-shell molecule (spin−orbit geometry optimizations on the Pu systems proved too computationally demanding). Calculations were performed both on the isolated molecule and including the effect of solvent, CH_2Cl_2, for both U and Pu. The addition of solvent had little effect on $An-O_{yl}$, with a slight reduction in $An-O_{TPPO}$ (ca. 0.05 Å) and a lengthening of the An−Cl bond. There was also an increase in P−O−An angle for both *cis* and *trans* isomers and reduction in Cl−An−Cl angle for the *cis* isomers. When we compare U with Pu, there is a reduction in all An−ligand distances from U to Pu, typically of 0.02−0.03 Å, as would be expected for six-coordinate An^{6+} with radii of 0.87 Å for U versus 0.85 Å for Pu.[22]

(16) Cohen, D. *J. Inorg. Nucl. Chem.* **1961**, *18*, 211.
(17) Infante, I.; Seveo, A.; Gomes, P.; Visscher, L. *J. Chem. Phys.* **2006**, *125*, 074301.
(18) Wester, D. W.; Sullivan, J. C. *Radiochem. Radioanal. Lett.* **1983**, *57*, 35.
(19) See, for example: (a) Tian, G.; Rao, L.; Oliver, A. *Chem. Commun.* **2007**, 4119. (b) Matsika, S.; Pitzer, R. M.; Reed, D. T. *J. Phys. Chem. A* **2000**, *104*, 11983.
(20) Bessonov, A. A.; Grigoriev, M. S.; Ioussov, A. B.; Budantseva, N. A.; Fedosseev, A. M. *Radiochim. Acta.* **2003**, *91*, 339.
(21) Balakrishnan, P. V.; Patil, S. K.; Sharma, H. D.; Venkatasetty, H. V. *Can. J. Chem.* **1965**, *43*, 2052.
(22) Shannon, R. D. *Acta Crystallogr.* **1976**, *A32*, 751.

Table 4. Relative Energy Differences (kJ mol^{-1}) between the *Cis* and *Trans* Forms of $[UO_2Cl_2(Ph_3PO)_2]$ and $[PuO_2Cl_2(Ph_3PO)_2]$ and Dipole Moments[a]

	(g), scalar	(s), scalar	(g), SO		(s), SO
		$[UO_2Cl_2(Ph_3PO)_2]$			
relative energy	−14.4	−3.2	−14.3	−14.6[b]	−3.4[b]
dipole moment *cis*	14.38	16.92	14.41	14.37[b]	16.91[b]
dipole moment *trans*	0.05	0.20	0.04	0.05[b]	0.20[b]
		$[PuO_2Cl_2(Ph_3PO)_2]$			
relative energy	−18.8	−3.5	−19.3[b]		−5.2[b]
dipole moment *cis*	9.60	15.27	9.73[b]		14.08[b]
dipole moment *trans*	0.10	0.07	0.10[b]		0.15[b]

[a] Negative relative energy values mean that the trans form is the more stable; (g) indicates isolated molecule; (s) indicates solvent-corrected molecule; SO indicates spin-orbit. [b] Data from single point calculations at the scalar geometry.

On comparison of the calculated data for the *cis* and *trans* complexes, the An−O_{yl} bond length is largely unaltered, with the An−O_{TPPO} shorter and An−Cl length longer in the *trans* derivatives. Presumably the An−O_{TPPO} bonds are longer in the *cis* derivatives due to the two bulky phosphineoxide ligands being adjacent. In solvent, these bond length changes are smaller than in the isolated molecules, perhaps because the P−O−An angle is bigger in solvent (for both *cis* and *trans*) and thus the bulk of the Ph groups is less critical. The O_{yl}−An−O_{yl} angle is always smaller in the *cis* derivatives, as we noted in our previous paper for the phosphinimine compounds,[6] while the P−O−An angle is also always smaller in the *cis* versus the *trans* derivatives, presumably to get the R groups further apart.

Tables 1, 2, and 3 indicate that the calculations reproduce the experimental An−Cl distances well and slightly overestimate the distances to the yl oxygens (by ca. 0.03 Å). The calculated An−O_{TPPO} bond lengths are, as found previously,[6] ca. 0.1 Å longer than experiment, although the experimentally observed ca. 0.05 Å lengthening in these distances on going from the *trans* to the *cis* species is mirrored computationally.

For both U and Pu, the *trans* isomer is the more stable (see Table 4). This relative stability reduces significantly on going from isolated molecule to solvent, which is probably related to the much larger dipole moment of the *cis* complexes, as we discussed previously for *cis*-/*trans*-$[UO_2Cl_2(Cy_3PX)_2]$, where X = O/NH.[6] In comparison of U with Pu, the *trans* form is more stable than the *cis* by a larger amount in the Pu complexes than the U complexes. This would appear to be consistent with the primary coordination shell of the Pu system being more crowded owing to the shorter Pu−ligand distances noted above. The effects of spin−orbit coupling on the relative energies of the *cis* and *trans* isomers are small for both U and Pu (the scalar and spin−orbit data differ by at most 1.7 kJ mol^{-1} (Table 4) for the solvent-corrected Pu system) and give a slightly larger preference for *trans* over *cis*.

Table 5 gives the scalar relativistic partial atomic charges for the metal and O_{TPPO} in *cis*-/*trans*-$[AnO_2Cl_2(Ph_3PO)_2]$ (An = U/Pu), both isolated and solvent-corrected molecules. It may be seen that the charge on the Pu atom is slightly more positive than that on the U in all cases and that the charge on the O_{TPPO} is always slightly more negative in the Pu complexes than in the U. If we take the charge difference between the metal and oxygen as a measure of the ionicity of the bond, we can conclude that the Pu−O_{TPPO} bond is more ionic than the U−O_{TPPO}. This is in keeping with the generally accepted

Table 5. Hirshfeld Atomic Charges, *q*, for the Metal and O_{TPPO} for the *Cis* and *Trans* forms of $[AnO_2Cl_2(Ph_3PO)_2]$ (An = U, Pu) [a]

	q_M (g)	q_O (g)	q_M (s)	q_O (s)	Δq (g)	Δq (s)
			$[UO_2Cl_2(Ph_3PO)_2]$			
trans	0.61	−0.26	0.60	−0.27	0.87	0.87
cis	0.60	−0.26	0.59	−0.27	0.86	0.87
			$[PuO_2Cl_2(Ph_3PO)_2]$			
trans	0.65	−0.28	0.64	−0.28	0.93	0.92
cis	0.64	−0.28	0.63	−0.28	0.92	0.91

[a] All calculations are scalar; (g) indicates isolated molecule; (s) indicates solvent-corrected molecule.

view of the bonding in actinide complexes (especially those with hard donor ligands), which holds that the bonding becomes increasingly ionic as the series is crossed.

It is clear that *trans*-$[PuO_2Cl_2(Ph_3PO)_2]$ is the major initial product and *cis*-$[PuO_2Cl_2(Ph_3PO)_2]$ is the minor product from the reaction between PuO_2Cl_2(aq) and Ph_3PO, when generation of Pu^{VI} from a Pu^{IV} stock is undertaken by ozonolyis (see Experimental Section for more details). The same products can be obtained when PuO_2Cl_2(aq) is generated via oxidation with Ag^{II} in perchlorate media, as confirmed by ^{31}P NMR spectroscopy. However, on several occasions the precipitated solids contained major impurities, as evidenced by solution-state spectroscopies. UV/vis/nIR spectra (in wet CH_2Cl_2) revealed two higher intensity transitions in the 800−900 nm region (840 and 851 nm) indicative of the $^3H_{4g} \rightarrow {}^3\Pi_{2g}$ transition for two complexes for which there is no inversion center at Pu^{VI} (see Supporting Information). In addition, over time additional transitions could be observed, consistent with reduction to Pu^{IV}.[1,16] Room temperature ^{31}P NMR spectra could be very complex with numerous resonances observed between 50 and −170 ppm, including the two resonances at −132 and −145 ppm that could be attributed to *cis*-/*trans*-$[PuO_2Cl_2(Ph_3PO)_2]$. Additional peaks observed at −94, −73, and −53 ppm probably correspond to additional Pu^{VI}−Ph_3PO complexes, including perhaps $[PuO_2(Ph_3PO)_4]^+$. A peak at 31 ppm could also be observed, which could be attributed to uncomplexed Ph_3PO or $[PuCl_2(Ph_3PO)_4]$ (see later discussion). This complex solution phase speciation led to the crystallization of two further minor products, the previously structurally characterized perchlorate salt, $[PuO_2(Ph_3PO)_4][ClO_4]_2$,[12] and *cis*-$[PuCl_4(Ph_3PO)_2]$. Crystallization of the former complex clearly shows that the carry through of perchlorate from the preparation of Pu^{VI} can alter reactivity while crystallization of the latter product confirms partial reduction to Pu^{IV} in solution. Unfortunately, the difficulties involved with undertaking ^{239}Pu research inhibited our attempts to systematically analyze in detail why different Pu^{VI} products could be formed from seemingly analogous reactions although clearly chemical impurities in the "PuO_2Cl_2" aqueous stock must play a role.

In *cis*-$[PuCl_4(Ph_3PO)_2]$, the central plutonium atom sits on a 2-fold rotation axis, with the asymmetric unit also comprising two chloride atoms and a Ph_3PO ligand, resulting in a molecule with two cis-coordinated Ph_3PO ligands and four coordinated chlorides. The analogous six-coordinate uranium(IV) complex is also known, crystallizing in the same *C*2/*c* space group.[23] The structure of *cis*-$[PuCl_4(Ph_3PO)_2]$ is shown

(23) Bombieri, G.; Brown, D.; Graziani, R. *J. Chem. Soc., Dalton Trans.* **1975**, 1873.

Table 6. Selected Bond Lengths (Å) and Angles (deg) for *cis*-$[AnCl_4(Ph_3PO)_2]$, where An = Pu (This Work) and U (Ref [23])

	Pu	U		Pu	U
An−O_{TPPO}	2.221(4)	2.242(7)	O_{TPPO}−An−O_{TPPO}	89.2(2)	88.9(3)
An−Cl	2.570(2)	2.609(4)	Cl−An−Cl	90.6(1), 89.7(1), 97.4(1)	90.4(1), 90.6(1), 97.5(1)
	2.572(2)	2.626(3)	O_{PH_3PO}−An−Cl (*cis* only)	90.3(1), 85.0(1), 87.9(1)	90.5(2), 88.1(2), 83.9(2)
P−O	1.520(4)	1.524(7)	An−O−P	163.6(2)	165.1(5)

in Figure 5, with selected bond lengths and angles given in Table 6.

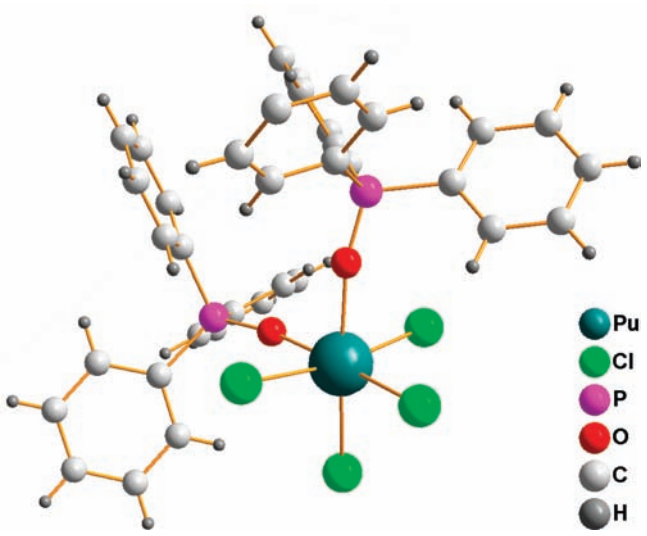

Figure 5. Ball and stick structural representation of *cis*-$[PuCl_4(Ph_3PO)_2]$.

Unsurprisingly the actinide coordination environments in *cis*-$[PuCl_4(Ph_3PO)_2]$ and *cis*-$[UCl_4(Ph_3PO)_2]$ are almost identical, with the only major difference being the shorter actinide−chloride bonds in the Pu complex (average 2.571 Å) compared with those in the uranium complex (average 2.618 Å). This is consistent with the slightly smaller ionic radii of six-coordinate Pu^{IV} (0.86 Å) versus U^{IV} (0.89 Å).[22] In contrast to Pu^{IV} and U^{IV}, a seven-coordinate Th^{IV} complex has been structurally characterized with an additional coordinated Ph_3PO ligand, $[ThCl_4(Ph_3PO)_3]$.[24] It would not be unreasonable to suggest that the larger ionic radius Th^{IV} center (0.94 Å) is the reason for the increased coordination number.[22] The significantly shorter Pu−Cl and Pu−O_{TPPO} bonds in *cis*-$[PuCl_4(Ph_3PO)_2]$ versus *trans*-$[PuO_2Cl_2(Ph_3PO)_2]$ appear to be counter-intuitive when compared with the smaller ionic radius of six-coordinate Pu^{VI} versus Pu^{IV} (0.85 versus 1.00 Å). However, the +VI charge on [*trans*-$PuO_2Cl_2(Ph_3PO)_2$] is partially quenched by the two plutonyl oxygens, Z_{eff} probably somewhere between +3.0 and 3.3,[24] and thus the Pu^{IV} center has a larger positive effective charge. This larger effective charge leads to stronger complexation to An^{IV} versus $\{AnO_2\}^{2+}$ for the majority of ligands where the influence of steric effects is minimal[25] and probably at least partly contributes to the shorter Pu−Cl and Pu−O_{TPPO} bonds in *cis*-$[PuCl_4(Ph_3PO)_2]$ versus *trans*-$[PuO_2Cl_2(Ph_3PO)_2]$. In addition, the closest hydrogen bonding interactions between a phenyl hydrogen and a chlorine atom of adjacent *cis*-$[PuCl_4(Ph_3PO)_2]$ molecules is 2.86 Å.

The ^{31}P NMR of *cis*-$[PuCl_4(Ph_3PO)_2]$ dissolved in CD_2Cl_2 revealed just one peak at 33.5 ppm, which could be attributed to either the dissolved complex or uncomplexed Ph_3PO. If indeed the peak is due to Ph_3PO then it can be assumed that in this complex paramagnetic broadening due to the close proximity of the phosphorus atoms to Pu^{IV} ($5f^4$) has resulted in the signal for the complex being indistinguishable from the baseline.

Our attempt to extend $PuO_2Cl_2L_2$ chemistry to L = Ph_3PNH, a moisture-sensitive ligand, requires a moisture-free synthetic entry route to the chemistry. We have therefore attempted to take advantage of the recently reported moisture-free plutonyl chloride complex $[PuO_2Cl_2(thf)_2]_2$.[11] However, the reaction between Ph_3PNH and $[PuO_2Cl_2(thf)_2]_2$ yielded only $[Ph_3PNH_2]_2[PuO_2Cl_4]$ as a crystalline product, as revealed by single-crystal X-ray diffraction. The anion, $[PuO_2Cl_4]^{2-}$, has previously been structurally characterized by Wilkerson et al., as the dicesium salt,[12] and is composed of the classical linear O−Pu−O actinyl moiety surrounded by four chloride ligands in the equatorial plane (D_{4h} symmetry). The Pu−O (1.709(10) and 1.718(9) Å) and Pu−Cl (2.641(4)−2.661(4) Å) bond lengths and O−Pu−O (178.6(4)°), O−Pu−Cl (88.2(3)−91.7(3)°) and Cl−Pu−Cl (85.71(11)−93.95(11)°) angles are all comparable to those reported by Wilkerson et al.[12] There are two crystallographically distinct $[Ph_3PNH_2]^+$ cations, with the two P−N bond distances (1.624(11)−1.625(11) Å) the same, within errors, as the values obtained for the P−N bonds in $[H_2NPPh_3]_2[OsCl_6]\cdot 2CH_3CN$ (1.627(9) and 1.64(1) Å).[26] The phosphonium cations interact with the $[PuO_2Cl_4]^{2-}$ anion through N−H···Cl hydrogen-bonding interactions, with each chloride ligand interaction with a different phosphonium hydrogen atom (one short, 2.08 Å, and three long, 2.52, 2.56, and 2.54 Å, interactions in total). Through these interactions, the phosphonium cations bridge the $[PuO_2Cl_4]^{2-}$ anions leading to the formation of infinite chains (see Figure 6).

The reaction between 4 mol equiv of Ph_3PNH and $[PuO_2Cl_2(thf)_2]_2$ was then probed in solution by both vis/nIR (CH_2Cl_2) and ^{31}P NMR (CD_2Cl_2) spectroscopies. It would be expected that the solution vis/nIR spectra of $[PuO_2Cl_2(Ph_3PO)_2]$ and $[PuO_2Cl_2(Ph_3PNH)_2]$ would be similar, assuming comparable ratios of *cis*/*trans* isomers. The vis/nIR spectrum of $[PuO_2Cl_2(Ph_3PO)_2]$ and that of 4 mol equiv of Ph_3PNH and $[PuO_2Cl_2(thf)_2]_2$ do indeed have many similarities (Figure 7), albeit with an apparent red shift of the major transitions in the latter spectrum. However, the solution spectrum of 4 mol equiv of Ph_3PNH added to $[PuO_2Cl_2(thf)_2]_2$ did not change during the 2 days following preparation and exposure of the sealed sample vial (under inert atmosphere) to air on the third day resulted in the appearance of a sloping baseline (see Supporting Information). This all points to the rapid decomposition of Ph_3PNH in the reaction solution and formation of one or more

(24) Van Den Bossche, G.; Rebizant, J.; Spirlet, M. R.; Goffart, J. *Acta Crystallogr.* **1988**, *C44*, 994.
(25) Choppin, G.R.; Jensen, M. P. In *The Chemistry of the Actinide and Transactinide Elements*; Morss, L. R.; Edelstein, N. M.; Fuger, J., Eds.; Springer: Dordrecht, The Netherlands, 2006; Vol. 4, Chapter 23, p 2524.
(26) Neumüller, B.; Dehnicke, K. *Z. Anorg. Allg. Chem.* **2007**, *633*, 841.

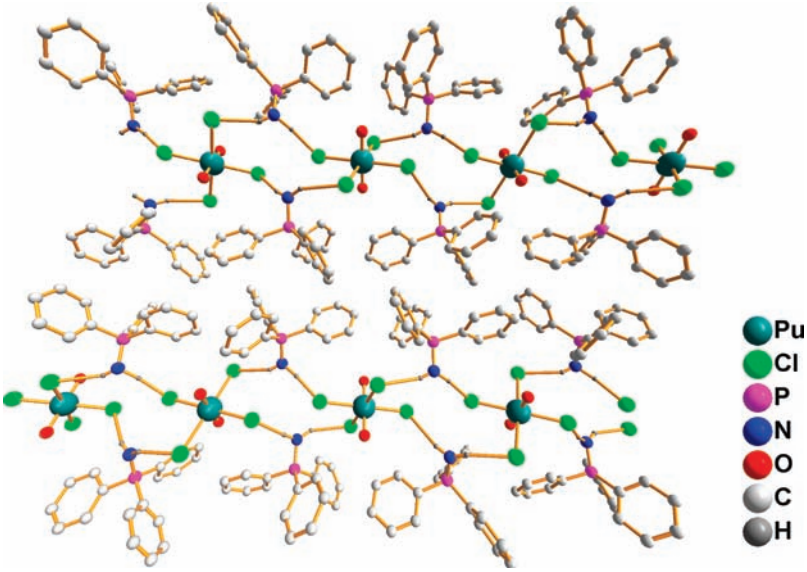

Figure 6. View down the *b* axis of $[Ph_3PNH_2]_2[PuO_2Cl_4]$ showing the hydrogen bonding between the N−H protons of the $[Ph_3PNH_2]^+$ cations and the Cl atoms on $[PuO_2Cl_4]^{2-}$.

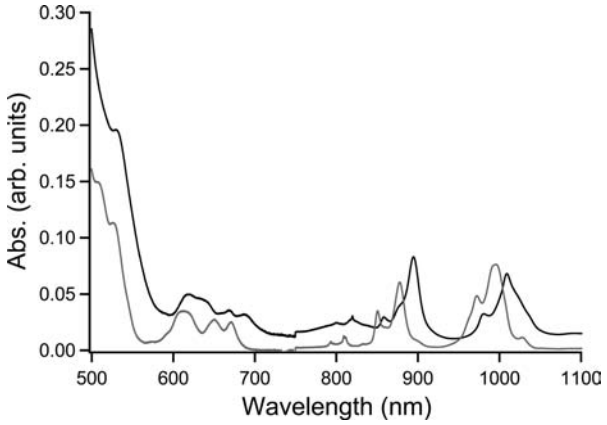

Figure 7. Vis/nIR spectra of $[PuO_2Cl_2(Ph_3PO)_2]$ (gray) and $[PuO_2Cl_2(thf)_2]_2$ + 4 mol equiv of Ph_3PNH (black).

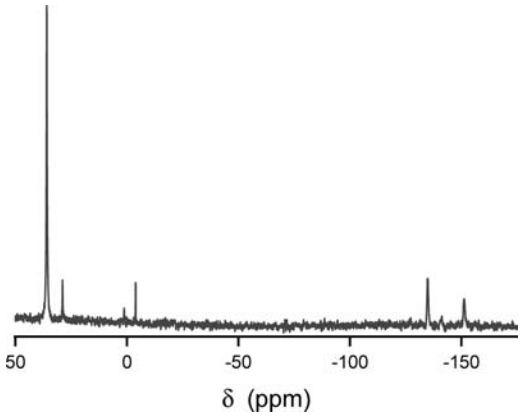

Figure 8. $^{31}P\{^1H\}$ spectrum of $[PuO_2Cl_2(thf)_2]_2$ + 4 mol equiv of Ph_3PNH in CD_2Cl_2.

solution plutonyl(VI) species with ligands that do not include coordinated phosphinimine. However, in common with the spectrum for $[PuO_2Cl_2(PPh_3PO)_2]$, there is no dominant 5f−5f ($^3H_{4g} \rightarrow {}^3\Pi_{2g}$) transition between 800 and 900 nm. This suggests that the major $\{PuO_2\}^{2+}$ complex present in solution has a coordination environment that has an inversion center, and it is pertinent to note that $[PuO_2Cl_4]^{2-}$ has an inversion center. In addition, if the solution mainly contains $[PuO_2Cl_4]^{2-}$, then the red shift of the main spectral bands versus those of $[PuO_2Cl_2(Ph_3PO)_2]$ is consistent with the red shift in absorption bands observed by Day and Venanzi for the vis/nIR spectra of $[Ph_3BuP]_2[UCl_6]$ versus $UCl_4(Ph_3PO)_2$ (i.e., a comparison of isoelectronic, $5f^2$, U^{IV} and Pu^{VI}).[27] The sloping baseline on exposure to air is attributed to the presence of trace solid suspension or colloid formation, perhaps due to either further ligand decomposition or partial reduction of the Pu^{VI} solution to hydrolyzed Pu^{IV}.

In the presence of moisture, Ph_3PNH will hydrolyze to yield Ph_3PO and NH_3. By ^{31}P NMR, we have observed the decomposition of Ph_3PNH to Ph_3PO in CD_2Cl_2, following the peak intensities of the phosphinimine (δ 22.3 ppm)[28] and phosphineoxide (28.8 ppm) resonances.[29] After 4 days, Ph_3PO was the dominant species with an additional minor product observed at −4 ppm, which can probably be assigned as Ph_3P.[29] However, the addition of 4 mol equiv of Ph_3PNH to $[PuO_2Cl_2(thf)_2]_2$ in CD_2Cl_2 led to a more complex RT ^{31}P NMR spectrum (see Figure 8). The major peak was observed at 35.9 ppm, which we assign to $[Ph_3PNH_2]^+$,[28] with minor resonances in the same region of the spectrum at 28.8 (Ph_3PO), 1.2, and −4.0 ppm (Ph_3P). We also observe peaks at −134.8 and −151.1 ppm. These latter two peak positions are comparable to the resonances observed for *cis*/*trans*-$[PuO_2Cl_2(Ph_3PO)_2]$ at 20 °C (−145.9 and −148.3 ppm), and we tentatively assign them to *cis*/*trans*-$[PuO_2Cl_2(Ph_3PNH)_2]$, indicating that there is at least some Ph_3PNH complexation to $\{PuO_2\}^{2+}$.

The structural and spectroscopic evidence points to Ph_3PNH protonation to $Ph_3PNH_2^+$ as the dominant chemical reaction

(27) Day, J. P.; Venanzi, L. M. *J. Chem. Soc. A* **1966**, 197.

(28) Abel, E. W.; Mucklejoner, S. A. *Phosphorus Sulfur* **1981**, *9*, 235. Hursthouse, M. B.; Walker, N. P. C.; Warrens, C. P.; Woollins, J. D. *J. Chem. Soc., Dalton Trans.* **1985**, 1043 and references therein.

(29) *Handbook of Phosphorus-31 Nuclear Magnetic Resonance Data* Tebby, J. C., Ed.; CRC Press: Boca Raton, FL, 1990.

when Ph_3PNH is reacted with $[PuO_2Cl_2(thf)_2]_2$, with the formation of $[PuO_2Cl_4]^{2-}$ as the major plutonium-containing product and *cis*/*trans*-$[PuO_2Cl_2(Ph_3PNH)_2]$ as minor products. The most likely source of protons and chloride is residual HCl/$SiMe_3Cl$, used in the preparation of $[PuO_2Cl_2(thf)_2]_2$, and perhaps the small scale of reaction (milligrams) prohibits the effective washing of this plutonium starting material. We have observed almost identical reactivity for the neptunium(VI) system, this time starting from $[NpO_2Cl_2(thf)]_n$,[30] which is at odds with the uranyl chemistry that we had hoped to mimic, that is, reaction of $[UO_2Cl_2(thf)_2]_2$ with 2 equiv of Ph_3PNH to form $[UO_2Cl_2(Ph_3PNH)_2]$.[5,6] Presumably the larger (multigram) scale synthesis of $[UO_2Cl_2(thf)_2]_2$ reduces the concentration of impurities, but there may also be an increased stability of $[NpO_2Cl_4]^{2-}$ and $[PuO_2Cl_4]^{2-}$ versus $[UO_2Cl_4]^{2-}$ that merits further exploration.

Conclusion

It is clear that there are many synthetic challenges and opportunities awaiting researchers who wish to explore the coordination chemistry of the plutonyl(VI) moiety with strong donor ligands. Our attempt to probe the chemistry of the plutonyl(VI) analogs of *cis*-/*trans*-$[UO_2Cl_2(Ph_3PO)_2]$ and *cis*-/*trans*-$[UO_2Cl_2(Ph_3PNH)_2]$ have met with mixed success. This is due to a combination of factors, which include Pu^{VI} redox instability, the smaller scale of reactions, and the apparent high stability of $[PuO_2Cl_4]^{2-}$. These results have thrown new light on this little explored area of transuranic coordination chemistry and provide yet more evidence that it is often unwise to rely on uranium chemistry as an analog to plutonium studies.

Experimental Section

Warning! *The ^{239}Pu used during the course of this research is a high specific activity α emitting radionuclide. Research with this isotope should only be undertaken in an appropriate radiochemical/nuclear facility.* In this case, experimental research was undertaken at both CEA, Marcoule, and at LANL. Aqueous solution manipulations were undertaken in a fume hood, and manipulations with air and moisture stable powdered samples were undertaken in a regular air atmosphere negative pressure box. The recrystallization of $[PuO_2Cl_2(Ph_3PO)_2]$ in CH_2Cl_2, all manipulations with Ph_3PNH, and many solution state spectroscopic preparations were undertaken in a negative-pressure helium atmosphere drybox. Multiple containment methods were employed for all spectroscopic and structural characterization. A detailed description of helium atmosphere drybox operations and the sample containment methodology have been described previously.[31]

^{239}Pu stock solutions were obtained from internal sources, with all other chemicals purchased from standard chemical suppliers apart from Ph_3PNH and $[PuO_2Cl_2(thf)_2]_2$, which were synthesized as described previously.[11,28,32]

Synthesis of $[PuO_2Cl_2(Ph_3PO)_2]$: Method 1. A Pu^{VI} stock in ca. 0.2 M HCl was prepared from a Pu^{IV} stock solution in nitric acid via ozonolysis, with details of this method described previously.[33] The complex could be formed by mixing $\{PuO_2\}^{2+}$ in ca. 0.2 M HCl with slightly greater than 2 mol equiv of Ph_3PO in acetone yielding a bright yellow precipitate under a yellow solution. Yellow/orange crystals of [*trans*-$PuO_2Cl_2(Ph_3PO)_2]\cdot(CH_3)_2CO$ suitable for single-crystal X-ray diffraction were grown from acetone by filtering the supernatant and storing at 5 °C overnight. The yield of $[PuO_2Cl_2(Ph_3PO)_2]$ could be maximized by cooling the aqueous/acetone solution to 5 °C for 2 h, pipetting off excess solvent, and allowing the initial crude product to dry. The solid could then be recrystallized from dry CH_2Cl_2 in an inert atmosphere glovebox at −35 °C. In a typical preparation, 21.1 mg (0.088 mmol) of Pu (as $\{PuO_2\}^{2+}$) in HCl yielded 54.3 mg (69%) of $[PuO_2Cl_2(Ph_3PO)_2]$.

Synthesis of $[PuO_2Cl_2(Ph_3PO)_2]$: Method 2. A Pu^{VI} stock in ca. 4 M HCl was prepared via the dissolution of freshly prepared Pu^{IV} hydroxides in a minimum of 4 M HCl and conc. $HClO_4$ (vol/vol ratio of 1:2.5). Ten molar equivalents of solid AgO was then added with stirring, and the resultant $AgClO_4$ precipitate was removed by filtration. Solid $NaHCO_3$ was then carefully added to the solution until a tan brown precipitate formed. The supernatant was removed; the solid was washed with H_2O and then redissolved in 4 M HCl yielding a solution of $\{PuO_2\}^{2+}$ in 4 M HCl, typically containing 90 mg of Pu. An aliquot of this solution when added to 2 mol equiv of Ph_3PO in acetone yielded a bright yellow precipitate under a yellow solution, as for method 1, although in this case, all the solid could be redissolved with crystals of the title compound forming after standing at room temperature for a couple of days.

Synthesis of *cis*-$[PuCl_2(Ph_3PO)_4]$. A solution of $\{PuO_2\}^{2+}$ (2.11 mg, 8.84×10^{-3} mmol Pu) in HCl (0.75 mL) was added to a solution of Ph_3PO (4.9 mg, 1.77×10^{-2} mmol) in 0.23 mL acetone. After 2 days, yellow crystals had deposited from the yellow solution.

Synthesis of $[PuO_2(Ph_3PO)_4](ClO_4)$. A solution of $\{PuO_2\}^{2+}$ (2.63 mg, 1.10×10^{-2} mmol Pu) in HCl was added dropwise to a solution of Ph_3PO (6.4 mg, 2.29×10^{-2} mmol) in 0.29 mL acetone. The resulting yellow solution was left to stand and 2 days later orange crystals had formed in the vial.

Reactions between $[PuO_2Cl_2(thf)_2]_2$ and Ph_3PNH. 1. Crystal Growth of $[Ph_3PNH_2]_2[PuO_2Cl_4]$. Thf (5 mL) was added to $[PuO_2Cl_2(thf)_2]_2$ (15.1 mg, 1.5×10^{-2} mmol) and Ph_3PNH (18.0 mg, 6.5×10^{-2} mmol), and the resultant cloudy orange solution was stirred for ca. 2 h. Cooling to −35 °C for 1 h did not noticeably increase the amount of precipitation, and thus the thf was removed *in vacuo*. The resultant solids were dissolved in the minimum amount of CH_2Cl_2 and then filtered through Celite to yield a deep orange solution, which was stored at −35 °C. After 9 days, a few block-shaped orange crystals had formed and single-crystal X-ray diffraction was used to confirm the structure of this crystalline material as $[Ph_3PNH_2]_2[PuO_2Cl_4]$.

2. Solution-State UV/vis/nIR Experiment. $[PuO_2Cl_2(thf)_2]_2$ (2.4 mg, 2.5×10^{-3} mmol) and Ph_3PNH (2.8 mg, 1.0×10^{-2} mmol) were dissolved, with stirring, in 1 mL of CH_2Cl_2, and the resultant solution was added to a quartz cuvette with a screw cap lid. Spectra were recorded on three consecutive days and then again after exposure to air. They were compared with the solution spectrum of $[PuO_2Cl_2(Ph_3PO)_2]$ (4.5 mg, 5.8×10^{-3} mmol), also dissolved in 1 mL of CH_2Cl_2.

3. Solution-State ^{31}P NMR Experiment. $[PuO_2Cl_2(thf)_2]_2$ (2.8 mg, 2.8×10^{-3} mmol) and Ph_3PNH (3.2 mg, 1.2×10^{-2} mmol) were dissolved, with stirring, in ca. 0.8 mL of CD_2Cl_2. The resultant cloudy solution was filtered through Celite into a PTFE insert NMR tube, which was then inserted into a standard glass NMR tube.

Spectroscopic Characterization. UV/vis/nIR spectra were recorded on either a Cary 6000i (solution state), a Cary 50

(30) Cornet, S. M.; Redmond, M. P., Collison, D., Sharrad, C. A.; Helliwell, M.; Warren, J. *C. R. Chim.*, in press.

(31) Gaunt, A. J.; Reilly, S. D.; Enriquez, A. E.; Scott, B. L.; Ibers, J. A.; Sekar, P.; Ingram, K. I. M.; Kaltsoyannis, N.; Neu, M. P. *Inorg. Chem.* **2008**, *47*, 29.

(32) Appel, R.; Hauss, A. *Angew. Chem.* **1959**, *71*, 626; *Chem. Ber.* **1960**, *93*, 405. Appel, R.; Köhnlein, G.; Schöllhorn, R. *Chem. Ber.* **1965**, *98*, 1355. Dehnicke, K.; Weller, F. *Coord. Chem. Rev.* **1997**, *158*, 103. Shtepanek, A. S.; Tochilkina, L. M.; A.V, Kirsanov, A. V. *J. Gen. Chem. USSR Ed., Engl.* **1975**, *45*, 2085.

(33) Reilly, S. D.; Runde, W.; Neu, M. P. *Geochim. Cosmochim. Acta* **2007**, *71*, 2672.

(solution state), or a Cary 5 (solid state, diffuse reflectance) spectrometer. ^{1}H and ^{31}P $\{^{1}$H$\}$ NMR spectra of were recorded on a Bruker Avance 300 MHz spectrometer (^{31}P NMR spectra recorded at 121.5 MHz) or on an Oxford Varian 400 MHz spectrometer (^{31}P NMR spectra recorded at 162 MHz). ^{31}P NMR spectra were measured relative to H_3PO_4 (85%). To clarify solutions, they were passed through Celite prior to analysis. The infrared spectrum was collected for eight scans using a Bruker Equinox 55 ATR machine.

Single-Crystal X-ray Diffraction. Crystal data for [*trans*-$PuO_2Cl_2(Ph_3PO)_2$]·$2(CH_3)_2CO$ were collected on a Bruker Smart CCD. Chemical formula = $C_{42}H_{42}Cl_{12}O_6P_2Pu$, M_w = 1017.60, monoclinic space group, $P2_1/n$, a = 8.912(3) Å, b = 14.769(5) Å, c = 16.077(6) Å, α = 90°, β = 95.841(4)°, γ = 90°, V = 2105.2(13) Å^3, T = 141(2) K, Z = 2, Mo Kα radiation (λ = 0.710 73 Å), μ = 1.813 mm^{-1}, yellow block with crystal dimensions = 0.18 × 0.12 × 0.08 mm^3, ρ_{calcd} = 1.605 g cm^{-3}. Intensity data of 19 610 reflections were collected in the range $-10 \le h \le 10$, $-17 \le k \le 17$, $-19 \le l \le 19$, 3725 unique reflections (R_{int} = 0.0588), R_1 = 0.0354 (for 2828 reflections with $I \ge 2\sigma I$), wR_2 = 0.0760 (all data), GOF = 1.131, max/min residual electron density = +0.502/−0.960 e Å^{-3}. Crystal data for $[Ph_3PNH_2]_2[PuO_2Cl_4]$ were collected on a Bruker Smart CCD. Chemical formula = $C_{36}H_{34}Cl_4N_2O_2P_2Pu$, M_w = 972.39, monoclinic space group, $P2_1/n$, a = 16.684(5) Å, b = 14.516(4) Å, c = 16.943(5) Å, α = 90°, β = 116.037(3)°, γ = 90°, V = 3686.9(19) Å^3, T = 140(1) K, Z = 4, Mo Kα radiation (λ = 0.710 73 Å), μ = 2.199 mm^{-1}, orange block with crystal dimensions = 0.16 × 0.16 × 0.14 mm^3, ρ_{calcd} = 1.752 g cm^{-3}. Intensity data of 23 969 reflections were collected in the range $-20 \le h \le 20$, $-17 \le k \le 17$, $-19 \le l \le 20$, 6505 unique reflections (R_{int} = 0.1728), R_1 = 0.0703 (for 3371 reflections with $I \ge 2\sigma I$), wR_2 = 0.1306 (all data), GOF = 0.965, max/min residual electron density = +3.072/−1.838 e Å^{-3}. Crystal data for *cis*-$[PuCl_4(Ph_3PO)_2]$ were collected on a Nonius Kappa CCD area detector diffractometer. Chemical formula = $C_{36}H_{30}Cl_{14}O_2P_2Pu$, M_w = 940.34, monoclinic space group, $C2/c$, a = 13.9751(9) Å, b = 13.1612(10) Å, c = 20.2217(15) Å, α = 90°, β = 96.330(4)°, γ = 90°, V = 3696.7(5) Å^3, T = 293(2) K, Z = 4, Mo Kα radiation (λ = 0.710 73 Å), μ = 2.189 mm^{-1}, yellow prism with crystal dimensions = 0.22 × 0.16 × 0.08 mm^3, ρ_{calcd} = 1.690 g cm^{-3}. Intensity data of 10 053 reflections were collected in the range $-14 \le h \le 17$, $-15 \le k \le 16$, $-21 \le l \le +24$, 3630 unique reflections (R_{int} = 0.0557), R_1 = 0.0479 (for 2220 reflections with $I \ge 2\sigma I$), wR_2 = 0.0801 (all data), GOF = 0.884, max/min residual electron density = +1.764/−0.654 e Å^{-3}. The data were processed using the HKL package.[34] Absorption effects for all compounds were empirically corrected with the program MULABS.[35] The structure was solved by the heavy−atom method with SHELXS97 and subsequent difference Fourier-syntheses and refined by the full-matrix least-squares on F^2 with SHELXL97.[36] All non-hydrogen atoms were refined in the anisotropic approximation.

Computational Details. Density functional theory calculations were performed using the Amsterdam density functional (ADF) [ADF 2008.01, SCM, Theoretical Chemistry, Vrije Universiteit, Amsterdam, The Netherlands, http://www.scm.com] quantum chemistry package with the PBE generalized gradient approximation exchange correlation functional.[37] TZP zero-order regular approximation (ZORA) all electron basis sets were used on all atoms except C and H where DZP ZORA all electron basis sets were used. Relativistic effects were accounted for by the ZORA model including both scalar and spin−orbit terms. The spin-restricted approach was employed for all of the U calculations, and the spin-unrestricted approach was employed for the Pu systems. For the scalar Pu calculations, an excess of 2 spin α over spin β electrons was input, while for the spin−orbit Pu calculations, the noncollinear method was used. Solvent effects (dichloromethane) were included by the conductor-like screening model.

A standard set of parameters was adopted for the geometry optimizations, which were performed without symmetry constraints, in which the integration grid was set to 5.0, the SCF convergence criterion 10^{-7}, and the geometry convergence 10^{-3} au Å^{-1}. However, full SCF or geometry convergence was not obtained in all cases, and for some calculations the results were deemed insufficiently satisfactory for inclusion. Of those that are reported, all converged to the limits stated above, with the exception of the following. For scalar *cis*-$[UO_2Cl_2(Ph_3PO)_2]$, the lowest energy gradient obtained was 0.0019 and 0.0013 au Å^{-1} for the isolated molecule and solvent-corrected molecule, respectively. For scalar *cis*-$[PuO_2Cl_2(Ph_3PO)_2]$, the lowest energy gradient obtained was 0.0016 and 0.0017 au Å^{-1} for the isolated molecule and solvent-corrected molecule, respectively. For $[PuO_2Cl_2(Ph_3PO)_2]$, for which spin−orbit geometry optimizations proved intractable, single-point spin−orbit calculations were performed at the scalar geometries. For single-point spin−orbit isolated molecule calculations on $[PuO_2Cl_2(Ph_3PO)_2]$, the SCF converged to 3.4×10^{-6} and 6.1×10^{-5}, respectively, for the trans and cis compounds. For single-point spin−orbit solvent-corrected molecule calculations on $[PuO_2Cl_2(Ph_3PO)_2]$, the SCF converged to 2.0×10^{-6} and 6.0×10^{-5}, respectively, for the trans and cis compounds.

At the scalar optimized geometries of the Pu molecules, the compositions (Mulliken, %) of the α218a and α219a molecular orbitals (the 5f^2 electrons) were found to be as follows: isolated molecule, trans, α218a 88 f_{xyz}, 6 $f_{z(x^2-y^2)}$, 2 f_{z^2y}, and α219a 51 f_{z^2y}, 27 $f_{y(3x^2-y^2)}$, 3 f_{xyz}, 2 $f_{x(x^2-3y^2)}$, 1 f_{z^3}; isolated molecule, cis, α218a 37 f_{z^2x}, 27 $f_{x(x^2-3y^2)}$, 25 f_{xyz}, 4 f_{z^3}, 3 f_{z^2y}, 2 $f_{z(x^2-y^2)}$, and α219a 38 f_{z^3}, 33 $f_{y(3x^2-y^2)}$, 4 f_{z^2x}, 3 f_{z^2y}, 2 $f_{x(x^2-3y^2)}$, 1 f_{xyz}, 1 f_{z^3}; solvent-corrected molecule, trans, α218a 79 f_{xyz}, 7 f_{z^2x}, 5 $f_{z(x^2-y^2)}$, 4 f_{z^2y}, 2 $f_{y(3x^2-y^2)}$, 1 f_{z^3}, and α219a 37 f_{z^2y}, 29 $f_{y(3x^2-y^2)}$, 7 f_{xyz}, 1 f_{z^2y}, 13 f_{z^3}; solvent-corrected molecule, cis, α218a 54 f_{z^2x}, 35 $f_{x(x^2-3y^2)}$, 6 f_{xyz}, 2 f_{z^3}, and α219a 45 f_{z^3}, 37 $f_{y(3x^2-y^2)}$, 2 $f_{z(x^2-y^2)}$, 1 f_{z^2x}, 1 f_{z^3}.

Acknowledgment. We acknowledge the Heavy Element Chemical Research Program, Chemical Sciences Division of the Office of Basic Energy Sciences, United States Department of Energy, the EPSRC (and specifically grants GR/S95169/01, GR/S06233/01, and GR/595152/01) and the EU ACTINET program for funding. We also thank UCL for computing resources via the Research Computing "Legion" cluster and associated services.

Supporting Information Available: Vis/nIR $[PuO_2Cl_2(Ph_3PO)_2]$ dissolved in wet CH_2Cl_2, vis/nIR spectra of $[PuO_2Cl_2(thf)_2]_2$ with 4 mol equiv of Ph_3PNH (blue), and crystallographic data in cif format. This material is available free of charge via the Internet at http://pubs.acs.org.

(34) Otwinowski, Z.; Minor, W. *Macromol. Crystallogr., Part A* **1997**, *276*, 307.

(35) Spek, A. L., *PLATON: Multi-purpose Crystallographic Tool*; University of Utrecht: the Netherlands, 1998.

(36) Sheldrick, G. M. SHELXL-97 and SHELXS-97, University of Göttingen, Göttingen, Germany, 1996.

(37) Perdew, J. P.; Burke, K.; Ernzerhof, M. *Phys. Rev. Lett.* **1996**, *77*, 3865. Perdew, J. P.; Burke, K.; Ernzerhof, M. *Phys. Rev. Lett.* **1997**, *78*, 1396.